Global and Planetary Change 247 (2025) 104743

Contents lists available at ScienceDirect

Global and Planetary Change

journal homepage: www.elsevier.com/locate/gloplacha

The Reef Island Geomorphic Activity Assessment: A new approach to quantify cay geomorphic change

Emily Lazarus [a,*], Stephanie Duce [a], Stephen Lewis [b], Scott Smithers [a]

[a] Earth and Environmental Sciences, College of Science and Engineering, James Cook University, Townsville, Queensland 4811, Australia
[b] Catchment to Reef Research Group, Centre for Tropical Water and Aquatic Ecosystem Research, James Cook University, Townsville, Queensland 4811, Australia

ARTICLE INFO

Editor: Jed O Kaplan

Keywords:
Great Barrier Reef
Geomorphology
Shoreline change
Morphodynamics
Digital shoreline analysis system

ABSTRACT

Cays (low-lying reef islands) are dynamic, unconsolidated sedimentary landforms which adjust their shape and position on a reef in response to hydrodynamic conditions and sediment supply. Quantifying meaningful cay geomorphic change is necessary to understand their natural variability and detect change patterns and trajectories. Shoreline movements on cays have been quantified globally using the Digital Shoreline Analysis System (DSAS) which records shoreline movements at regularly spaced shore-normal transects. However, DSAS was developed for relatively straight coasts and is less suited to cays which have 360° shorelines. Here we introduce the Reef Island Geomorphic Activity Assessment (RIGAA), an alternative approach to quantify changes to cay area and shape, orientation, and position that uses the entire cay footprint. To compare the RIGAA to the DSAS, we used digitised cay shorelines captured monthly for three cays on the Great Barrier Reef to quantify cay geomorphic change over almost a decade (2015–2023). Both approaches yield comparable assessments of net cay shoreline change but the DSAS overall Net Shoreline Movement metric suggests progradation (4.14–13.12 m) dominates at all cays whereas the RIGAA indicates more diverse behaviours, including shoreline contraction (Taylor Cay −32.8 %), expansion (Bushy Islet +22.9 %) and stability (Masthead Island +2.9 %). The RIGAA approach accounts for the frequency and magnitude of shoreline perturbations and provides a comprehensive assessment of cay morphodynamic behaviour applied to the entire cay footprint. The outputs provide meaningful metrics for a range of users, including key information about overall cay area and morphological change, and movement.

1. Introduction

Coral cays are low-lying reef islands composed of largely unconsolidated carbonate sediment deposited on reef surfaces that dynamically adjust their shape and position on the reef in response to changes in hydrodynamic and sediment supply processes (Gourlay, 1988). There is widespread concern that anthropogenic pressures associated with climate change (e.g., sea-level rise, changed storm exposure, and modified sea-surface temperature and ocean pH which reduce calcification and modify biogenic sediment budgets) will force changes to cay morphology (size, shape, elevation) and morphodynamics (frequency, magnitude and timing of changes in cay shoreline and position on reef) that diminish their capacity to support critical ecosystem and cultural services (Kennedy, 2024). Reef island research to date has largely concentrated on mid-ocean atoll settings (Costa et al., 2017; Duvat, 2019; Ford, 2012; Kench and Brander, 2006; Kench et al., 2023; Purkis et al., 2016; Sengupta et al., 2021). Few studies have examined potential changes on cays formed on reef platforms developed on continental shelves, such as those of the Great Barrier Reef (GBR), Australia, which are exposed to different environmental conditions and may respond very differently to their mid-ocean counterparts (Dawson, 2021). Systematically measuring and quantifying the morphodynamic behaviour of cays is a critical step in better understanding the nature of cay dynamics and variability over different timescales (episodic, seasonal, interannual and decadal), and for detecting trends that may require a management response. In this paper we focus on cays which are predominantly located on the leeward margins of platform reefs, and are found in locations such as the GBR (Steers, 1929), Indonesia (Umbgrove, 1928) and the Caribbean (Stoddart, 1962) but the methods presented are applicable to islands in other contexts.

Cay morphodynamic analysis began as field mapping, including topographic profiles (e.g., Stoddart et al., 1978) or tracing aerial

* Corresponding author.
E-mail address: emily.lazarus@my.jcu.edu.au (E. Lazarus).

https://doi.org/10.1016/j.gloplacha.2025.104743
Received 29 September 2024; Received in revised form 6 February 2025; Accepted 7 February 2025
Available online 8 February 2025

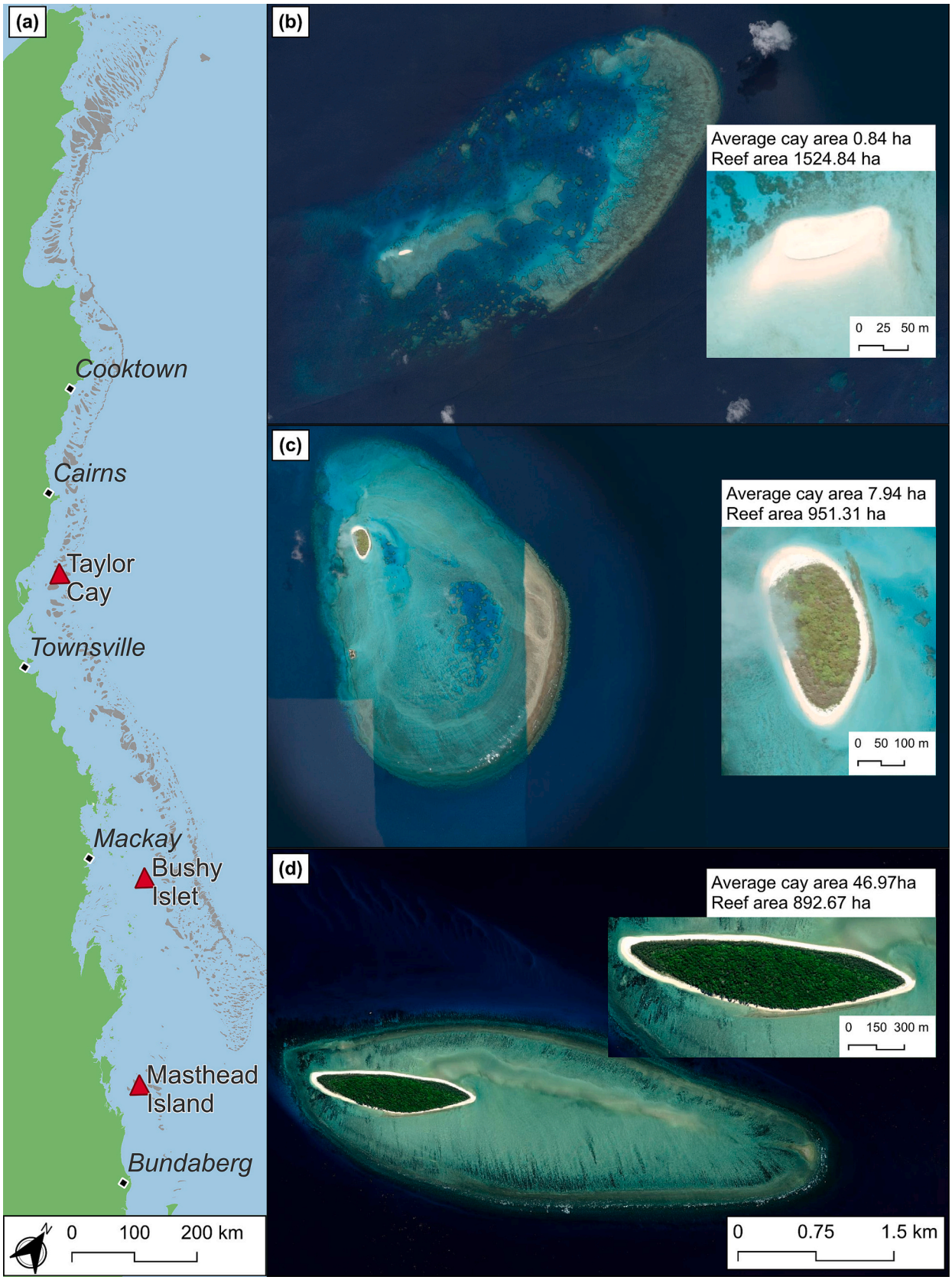

Fig. 1. An overview of the broader GBR context and (a) the location of the study cays with respect to the north-eastern Australian coastline, as well as the average cay area over the study period and reef platform area for (b) Taylor Cay, (c) Bushy Islet, and (d) Masthead Island.

photographs (e.g., Flood, 1974) which were captured sporadically. Following the widespread accessibility and increased recapture frequency of satellite imagery over the past few decades, cay morphodynamic analysis can now be undertaken on a near-monthly to weekly basis using emerging geospatial technologies, some of which are semi-automated (e.g., Cuttler et al., 2020) or automated (e.g., Bishop-Taylor et al., 2021). These new, vastly larger datasets are more powerful, requiring new methods of analysis to unlock their potential. In the past cay morphodynamic behaviour has mostly been assessed by measuring distances and rates of change to shoreline position at regularly spaced transects using the Digital Shoreline Analysis System (DSAS), an extension to ArcMap (Holdaway and Ford, 2019). While this approach has been usefully applied to numerous reef islands (e.g., Adnan et al., 2016; Dawson, 2021; Duvat and Pillet, 2017; Ford, 2013; Husband et al., 2023; Mann and Westphal, 2016), DSAS was primarily developed to analyse relatively straight coastlines (Himmelstoss et al., 2018) with each transect assessing only one dimensional (cross-shore) change (Shope and Storlazzi, 2019). This is not well suited to capture to the cross-shore and alongshore sediment exchanges around continuous, 360° reef island shorelines (Kench and Brander, 2006; Paris and Mitasova, 2014; Smithers and Dawson, 2023). Some limitations of DSAS include: 1) transects do not account for total planimetric change as transect spacing does not capture the entire cay shoreline; 2) island migration (i.e., change in overall location) is not well-captured or intuitively presented; 3) the user is required to indicate an appropriate baseline from which changes in distance are measured which is not necessarily appropriate for highly dynamic islands; 4) change is measured as distances or rates at each transect which are not directly or intuitively comparable to ecosystem services (e.g., sea bird or turtle nesting, habitable land) which are often best quantified by area; 5) it is difficult to summarise DSAS outputs into a meaningful, island-scale metric that can be compared between multiple islands (e.g., to help managers prioritise resources); and 6) requires paid software (ArcMap), although a free version for use with QGIS is now available (Terres de Lima et al., 2021).

Here we present the Reef Island Geomorphic Activity Assessment (RIGAA), an approach that uses free open-source software to: 1) quantify changes to cay shape and area; 2) enable temporal and spatial variability in cay shape and position to be determined, and identify zones of stability and high mobility; and 3) quantify the monthly cay orientation and migration over the reef platform. The outputs of RIGAA identify important attributes of cay morphodynamic behaviour, including key areas of change or instability, which can be intuitively displayed and understood by a diverse range of users. We compare the results of DSAS and RIGAA approaches applied to three cays on the GBR and demonstrate the benefits of the RIGAA approach.

2. Materials and methods

To demonstrate the use of the RIGAA we analysed the morphodynamics of three cays within the GBR. The cays were selected to capture some of the diversity of size, morphology and vegetative cover across a range of latitudinal, cross-shelf and hydrodynamic settings (Fig. 1a). The cays are Taylor Cay, a small (0.84 ha) unvegetated cay in the northern GBR; Bushy Islet, a medium (7.94 ha) vegetated cay in the central GBR; and Masthead Island, a large (46.97 ha) vegetated cay in the southern GBR (Fig. 1b, c and d, respectively). Direct anthropogenic modifications that may disrupt natural morphodynamic behaviour are absent from these cays. The analysis period extended from August 2015 to February 2023, beginning with strong El Niño conditions followed by a period of largely neutral to La Niña conditions (BOM, 2023) (See Supplementary Fig. S1).

Short- and long-term fluctuations in cay area, morphology, orientation and position on the reef platform must be known to fully define a cay's morphodynamic behaviour and start to understand its drivers. The Reef Island Geomorphic Activity Assessment (RIGAA) seeks to

Table 1
Summary of the definitions and interpretations of metrics measured by the Reef Island Geomorphic Activity Assessment (RIGAA).

Metric		Definition	Interpretation
Net cay change		Change in cay area between two discrete timesteps including identification of areas that have prograded, receded or remained relatively stable	This can inform the possible future trajectory of a cay by identifying the areas of contraction, expansion or relative stability, as well as estimating a net overall cay size trajectory to determine whether management intervention may be required (e.g., if net contraction is occurring).
Historical cay footprint intersection	*Historical cay positional envelope*	Aggregated area of all cay footprints for the observational period	Indicates the total area occupied by the cay for the observational period (including migration) to provide an estimate of the possible sediment exchange envelope/ storage capacity across the reef flat.
	Proportion of overlap	Percentage of cay footprints that overlapped at a given area as a proportion of the total number of cay footprints used in the analysis	Provide insight into the frequency at which various sections of the cay undergo change. When monthly footprints are used, as was the case in this study, these values can be interpreted as a proportion of time that the cay is present at a given position. This information can be used to inform management. For example, it would not be advisable to place a building or hard structure in an area with a low proportion of overlap. The suitability of certain areas for renourishment or grading could also be assessed based on the frequency of change.
	Maximum historical overlap	Identifies areas of overlapping cay footprints as a proportion of the historical cay positional envelope	Gives an indication of the stable proportion of the historical cay positional envelope. A high value suggests most of the cay is relatively stable while a low value shows the cay is more dynamic. This is a good metric to compare geomorphic activity between different islands and can give insight into the ongoing capacity of the cay to support ecosystem services, and thus, the need for management intervention.
Cay orientation		Measures the orientation of the cay long-axis in degrees from 0° (north)	Identify whether the orientation of the cay is changing in response to external forcings, and

(*continued on next page*)

Table 1 (*continued*)

Metric	Definition	Interpretation
		whether management intervention may be required to preserve ecosystem or cultural services.
Cay migration	Quantifies the change in cay centroid position over time relative to the position of the first timestep	Provides an estimate of whether the cay is migrating across its reef platform in response to external forcing conditions. This can inform a long-term trajectory of change.

characterise cay behaviour using the following metrics: 1) net cay change, 2) historical cay footprint intersection (including proportion of cay overlap and maximum historical overlap), and 3) cay orientation and migration as described below and summarised in Table 1.

2.1. Data acquisition

Monthly cay shoreline positions were used to compare the DSAS and RIGAA methods. The monthly shoreline positions were manually digitised by a single operator in ArcMap 10.8.2 from Sentinel-2 satellite imagery (10 m pixel resolution) at a 1:1000 scale (Fig. 2a). The vegetation line is commonly used as a shoreline proxy, however, the position of the toe of the beach (TOB) was instead chosen to apply a standardised method to unvegetated and vegetated cays. The TOB is defined by the break in slope from the cay shoreline to the reef flat, often associated with a change in sediment texture (Kench and Brander, 2006) and defines the most geomorphologically active section of cays (Costa et al., 2017). The area enclosed by the TOB is considered in this study to be the cay footprint (Fig. 2b).

Sentinel-2 image resolution (10 m) was sufficient to manually detect the TOB regardless of the tidal level. Given the size of the smallest cay on the GBR is approximately 60 m^2, Sentinel-2 imagery is at the threshold for manual shoreline detection. Additionally, the image recapture frequency of Sentinel-2 allowed near-monthly analysis which is an advancement on episodic aerial photos. This increased temporal resolution enabled us to capture the more subtle changes to cay geomorphic behaviour. Images where cloud cover obscured any part of the cay TOB were omitted resulting in some months being excluded from the analysis. Over the complete time series (August 2015 – February 2023, n = 91 months), the monthly images used in the analyses include Taylor Cay n = 83 (92 % of the study period); Bushy Islet n = 78 (87 %); and Masthead Island n = 86 (95 %) (Fig. 3a, b and c, respectively).

Positional uncertainty of the shorelines was calculated by the Root Mean Square Error (RMSE), taking the square root of the sum of the squared sources of error divided by the sample size (n) for each cay. The three sources of error considered were: 1) geolocation error of Sentinel-2 imagery (20 m (ESA, 2012)); 2) satellite image pixel size (10 m); and 3) human digitisation error (Husband et al., 2023). Human digitisation error was calculated by digitising the entire shoreline perimeter of each cay ten times from the same image and calculating the average variance of perimeter lengths. The overall RMSE was 2.41 m (Masthead Island), 2.45 m (Taylor Cay) and 2.53 m (Bushy Islet).

2.2. Digital Shoreline Analysis System

A mid-shore baseline (positioned between the most upper and lower shorelines) was digitised from the ESRI basemap. Transects were cast from the mid-shore baseline at 5 m intervals around the cay perimeters to measure the Net Shoreline Movement (NSM) and Shoreline Change Envelope (SCE). The NSM is the distance between the oldest and youngest shoreline positions and is calculated in metres (Himmelstoss et al., 2018). The SCE is the greatest distance of shoreline position movement along a transect, regardless of timing, and is calculated in metres (Himmelstoss et al., 2018). To enable a comparable analysis between RIGAA and DSAS at the island scale, the average value of NSM and SCE across all transects around a cay was used. Where the average NSM value for a cay was positive we classed this as showing cay expansion, while a negative average NSM value indicated cay contraction. We acknowledge that the use of an average value for each cay is not ideal as localised shoreline changes will be smoothed out and the overall value may be influenced by outliers. The difficulty calculating a single meaningful metric that characterises cay shoreline change is a limitation of the DSAS approach which our method seeks to overcome.

2.3. Reef Island Geomorphic Activity assessment

The RIGAA was undertaken using QGIS 3.22 where the digitised TOB lines were converted to polygons of the monthly cay footprint and the area calculated (ha) (Fig. 2b). The methods to obtain each of the metrics are detailed below, as well as a summary of the RIGAA metric definitions and interpretations in Table 1.

2.3.1. Net cay change

The net cay change was determined for each cay by performing a spatial union overlap analysis between two timesteps (Fig. 4). In this study, the oldest and most recent cay footprints were used; however, this metric can be adapted to analyse net change between any two timesteps.

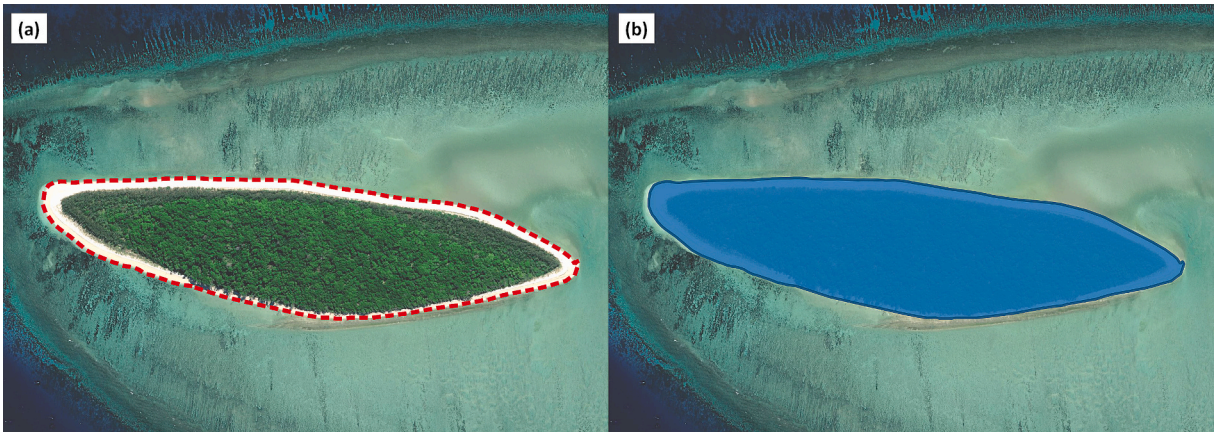

Fig. 2. Using Masthead Island as an example to compare (a) a linear shoreline manually digitised at the toe of beach (TOB) position as used for the DSAS approach and (b) the conversion to a cay footprint used in the RIGAA approach.

Fig. 3. The manually digitised monthly shorelines from the toe of beach (TOB) position displayed by year for (a) Taylor Cay (n = 83), (b) Bushy Islet (n = 78), and (c) Masthead Island (n = 86).

For example, it can be used to assess the impact of episodic events such as tropical cyclones (TCs) to determine the net change in cay area post-event. Additionally, for seasonal cay behaviour it could be used to identify change between a summer and winter cay footprint. This metric identified which areas of shoreline have prograded (net expansion), receded (net contraction) or remained relatively stable. The net cay change was calculated as the difference in cay area between the newest and oldest timesteps as a proportion of the area of the oldest cay footprint (1). Based on the approach established by Webb and Kench (2010), values above 3 % indicate net expansion, below −3 % indicate net contraction, and values in between indicate relative stability. It is important to note that this metric only takes into account the two shorelines selected for inclusion and therefore excludes any shoreline changes that occurred between these two timesteps.

$$\text{Net cay change} = \frac{\text{Area (new)} - \text{Area (old)}}{\text{Area (old)}} \times 100 \quad (1)$$

2.3.2. *Historical cay footprint intersection*

Three metrics capture the intersection of all cay footprints recorded over the observational period. The historical cay positional envelope is the total (aggregated) area occupied by all the cay footprints (Fig. 5a) over the observational period calculated using the Dissolve tool (Fig. 5b). The proportion of cay overlap was calculated using the Count Polygon Overlap Model (Jenkins, 2020) to determine the total number of cay footprints that overlapped at each area within the historical cay positional envelope (Fig. 5c). In the field calculator for each of the output overlap polygons a ratio of the number of intersecting cay footprints present in that area to the total number of cay footprints was

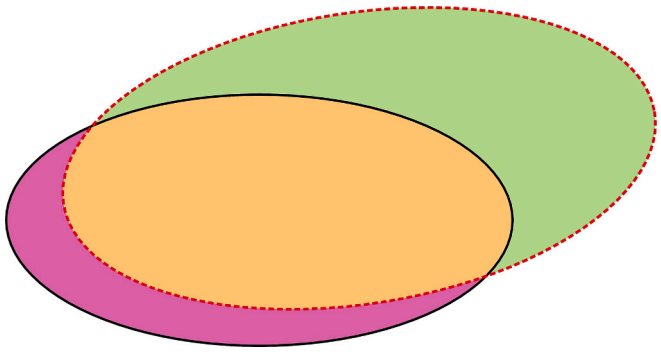

Fig. 4. A simplified example of the net cay change metric where the cay footprint of the first timestep is outlined in solid black and the second timestep is the dashed red outline. The areas of relative stability are shown by the orange shading (indicating the overlapping area between the two timesteps), the prograded area is shown in green, and cay shoreline recession shown by the pink shaded area.

calculated to determine the proportion (%) of overlapping footprints (Eq. 2).

To calculate the maximum historical overlap the area/s where all input cay footprints overlapped were identified. The proportion of the entire historical cay positional envelope covered by this area of maximum overlap was then calculated (Eq. 3, Fig. 5d). This gives the percentage of the historical cay footprint envelope which can be considered relatively stable or consistent. For highly mobile cays it is possible that there will be no area where all input footprints overlap (as was the case for Taylor Cay in our study). In such cases, the area with the greatest number of overlapping footprints can be used to calculate the maximum historical overlap. As with the net cay change, this metric can be adapted to measure seasonal intersections of cay footprints to characterise cay footprint perturbations relative to seasonal wind and wave conditions.

$$\text{Proportion of cay overlap} = \frac{\text{Number of intersecting cay footprints}}{\text{Total number of cay footprints}} \times 100$$

$$\text{Maximum historical overlap} = \frac{\text{Area where all footprints overlap}}{\text{Area of historical cay positional envelope}} \times 100$$

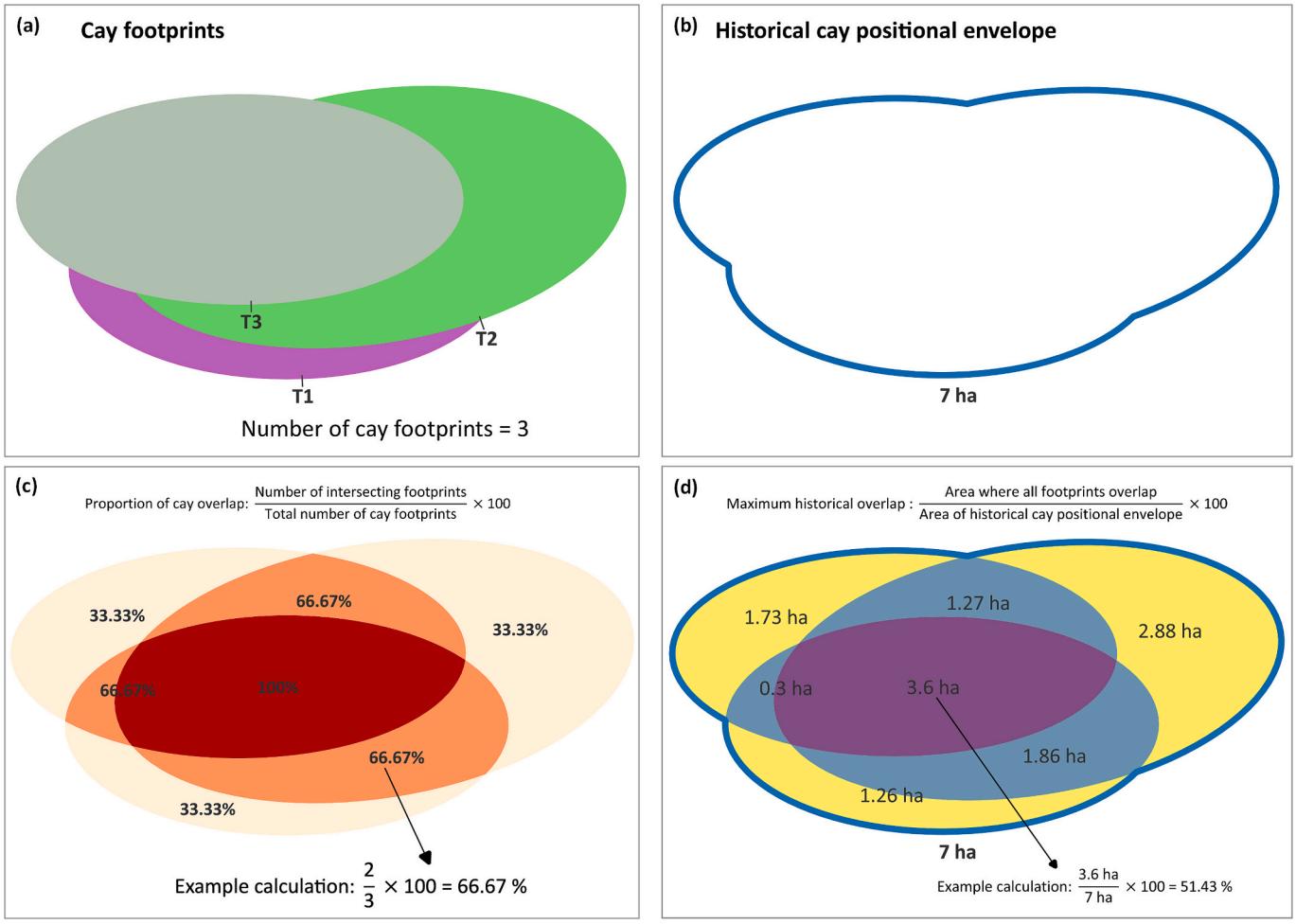

Fig. 5. The process of the historical cay footprint intersection from: (a) using the digitised cay footprints (based on three timesteps at T1, T2 and T3 as an example) to calculate (b) the historical cay positional envelope, then (c) determining the proportion of cay overlap, including an example calculation, and (d) determining the maximum historical overlap, including an example calculation.

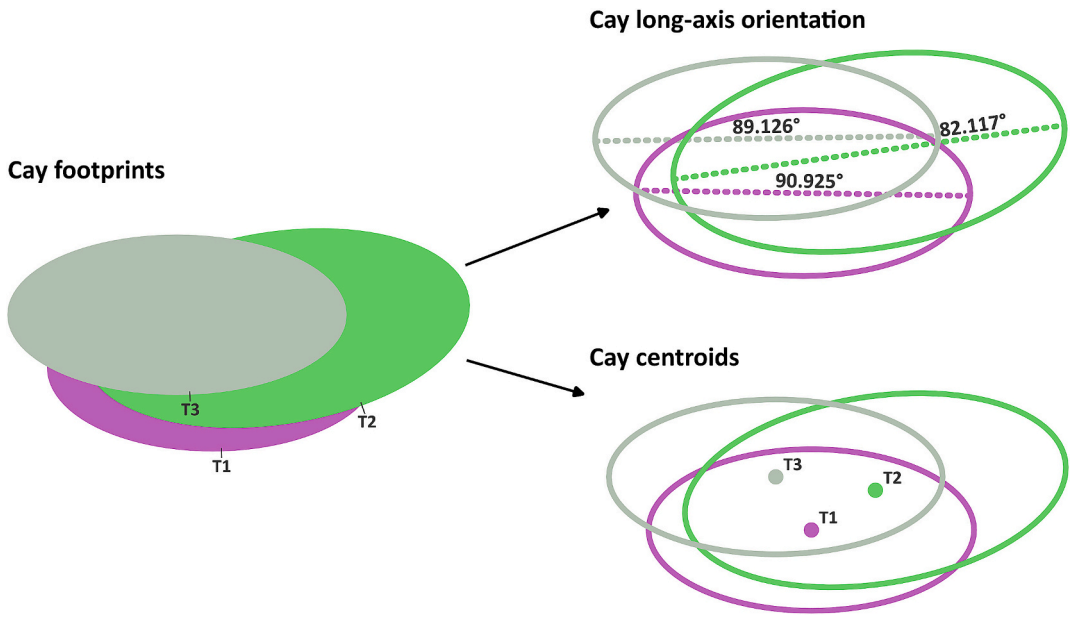

Fig. 6. The process of deriving the cay long-axis orientation (above right) and generating cay centroids (below right) from the digitised cay footprints (left).

2.3.3. Cay orientation and migration

Monthly cay orientation was calculated for the long axes derived from the footprints using the expression: *main_angle(geometry)* in the QGIS Field Calculator (Fig. 6). This function gives the bearing of the long-axis in degrees from north. Patterns of cay migration were measured by generating monthly centroid points from each cay footprint polygon (Fig. 6). Centroids were generated at the geometric centre of each polygon derived from the mass centre analysis method developed by Paris and Mitasova (2014) and applied to reef islands by Albert et al. (2016). The Distance to Nearest Hub (Points) tool was used to measure the distance of monthly cay centroid movement relative to the centroid position of the first timestep. The Align Points to Features tool was used to measure the monthly cardinal direction of centroid movement.

Rose diagrams were used to visualise the monthly long-axis orientation and cay centroid migration. Monthly cay long-axis orientation was plotted using the long-axis angle (degrees) and area (ha) of the monthly cay footprint. Centroid migration was plotted to visualise the monthly cardinal direction (degrees) and distance (m) measured relative to the first timestep. These measurements were plotted using the Python package '*plotly*'.

2.4. Comparing the methods

We compared the DSAS metric of average NSM to RIGAA's net cay change, and the average SCE (DSAS) to the RIGAA metrics proportion of overlap and maximum historical overlap. While we acknowledge that we cannot draw direct comparisons as the two methods use different units, these comparisons provide useful insights into the advantages and limitation of each approach. Net cay change was used to determine the extent of cay shoreline progradation (net expansion), recession (net contraction) or relative stability between two timesteps, which can be considered the first step in determining whether a cay may be changing or contracting in total area and require management intervention. The results of the historical cay footprint intersection enabled identification of sections of the cay which had undergone more frequent change and could be used to inform the suitability of management interventions. Finally, while there is no DSAS equivalent, we show how cay orientation and migration can be used to understand short-term movements due to extreme events, or the long-term response of a cay to external forcings, such as hydrodynamic conditions, and can be used to infer future trajectories.

3. Results and discussion

3.1. Net cay change

The NSM from DSAS and the net cay change metric from RIGAA identify the same locations of shoreline progradation, relative stability and recession (Fig. 7). However, different conclusions with respect to cay change are derived for the overall net cay change (RIGAA) and the average overall NSM (DSAS) (Table 2). The DSAS results indicate a net positive (expanding) change in average shoreline movement at all three cays, whereas the RIGAA indicates a net contraction of cay area (−32.8 %) and complete relocation at Taylor Cay, net expansion at Bushy Islet (22.9 %), and relative stability at Masthead Island (2.9 %). This discrepancy arises because the DSAS method does not accommodate changes in cay area or position on the reef platform (Mann et al., 2016). This phenomenon is best exemplified at Taylor Cay (Fig. 7a and b) where the RIGAA method shows that the cay has entirely relocated to the north while the DSAS method identifies high net shoreline progradation (up to 60 m) on the northern shore accompanied by moderate shoreline recession (10–30 m) on the southern shore, which is not intuitively interpreted as complete cay relocation. We emphasise that a reduction in cay area does not universally indicate net sediment loss from the cay (Lowe et al., 2019); the change may be the result of a temporary flux between the cay and proximal reef flat, or vertical accretion of the cay, which cannot be measured by either the DSAS or RIGAA methods. A three-dimensional assessment (e.g., using LiDAR or drone-derived structure from motion methods to create digital elevation models) of cay morphology and change over time is required to assess this (Hamylton, 2017; Lowe et al., 2019).

3.2. Historical cay footprint intersection

The SCE results (DSAS) identify the greatest fluctuation of shoreline position along the southern end of Bushy Islet (110–120 m) (Fig. 8c, Table 2) and western spit of Masthead Island (100–115 m) (Fig. 8e,

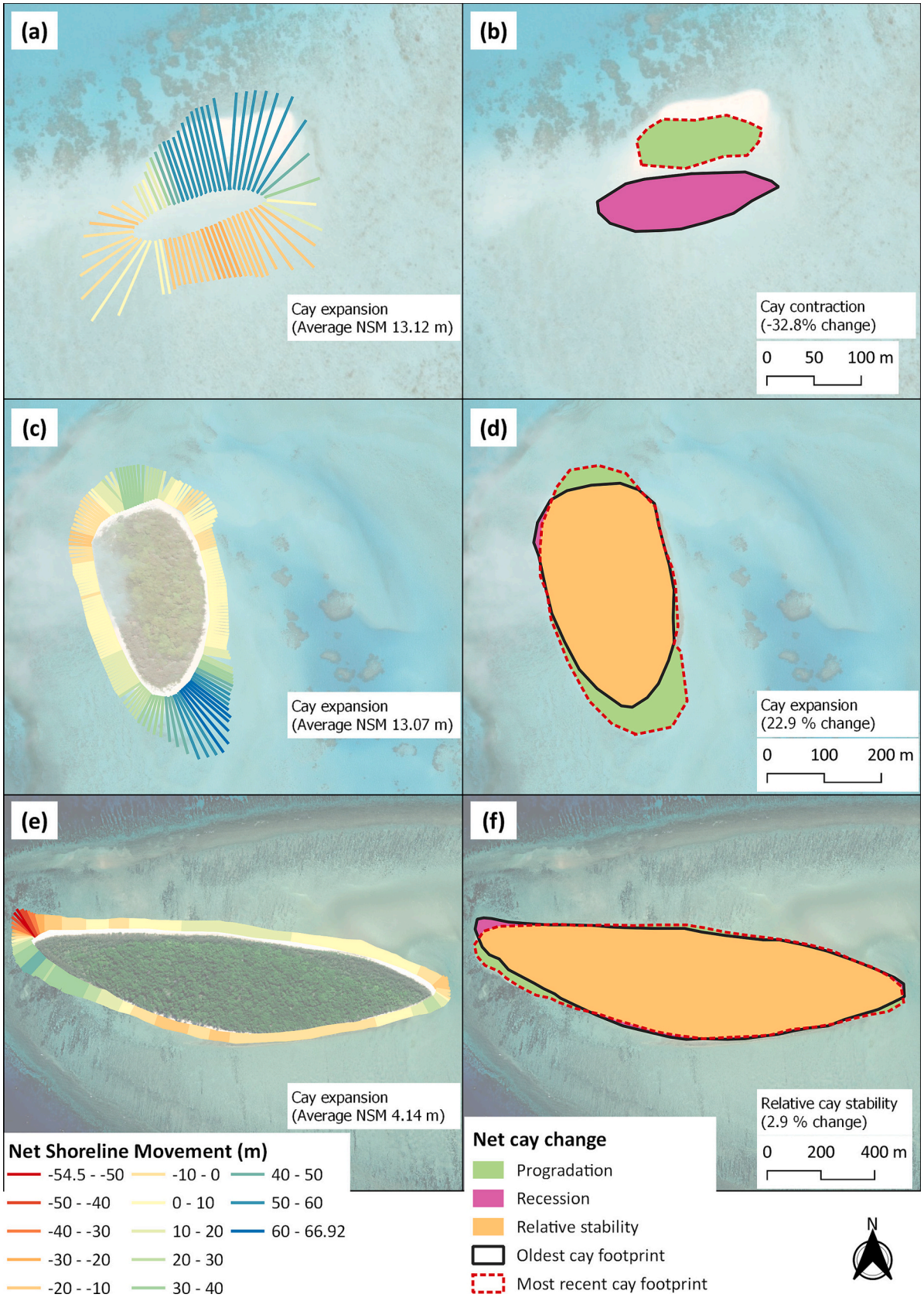

Fig. 7. Comparing the average Net Shoreline Movement (NSM) statistic at each transect calculated in DSAS and the net cay change results from the RIGAA, respectively, to measure planimetric cay area change at (a, b) Taylor Cay which completely relocated to the north, (c, d) Bushy Islet, and (e, f) Masthead Island.

Table 2
Quantitative summary of the results comparing the DSAS to RIGAA for all method metrics. The DSAS metrics are highlighted in blue and the RIGAA metrics are highlighted in orange. Note: that the two approaches are often not directly comparable given the different units of some metrics.

		Taylor Cay	Bushy Islet	Masthead Island
Net cay change	DSAS – Net shoreline movement (NSM)	Net cay expansion (overall average 13.12 m)	Net cay expansion (overall average 13.07 m)	Net cay expansion (overall average 4.14 m)
	RIGAA – Net cay change	Net contraction (-32.8 %)	Net expansion (22.9 %)	Relative stability (2.9 %)
Historical cay footprint intersection	DSAS – Shoreline change envelope (SCE)	Overall SCE average 63.5 m	Overall SCE average 39.9 m	Overall SCE average 33.2 m
	RIGAA – Proportion of overlap	Largest proportion of overlap 62.65 %	Largest proportion of overlap 100 %	Largest proportion of overlap 100 %
	RIGAA – Maximum historical overlap	Largest maximum historical overlap 3.2 %	Largest maximum historical overlap 56.9 %	Largest maximum historical overlap 78.1 %
Cay orientation	RIGAA – Cay orientation	Range of long-axis orientation 68-94°	Range of long-axis orientation 158-177°	Range of long-axis orientation 91-100°
Cay migration	RIGAA – Cay migration	Maximum distance of migration 121 m	Maximum distance of migration 32 m	Maximum distance of migration 30 m

Table 2). These positions coincide with the areas with the least proportion of overlap (0–20 %) when applying the RIGAA. However, the DSAS results do not indicate the temporal dynamics of these shoreline fluctuations, whereas the RIGAA proportion of overlap offers a measure of the frequency of these fluctuations. Given monthly cay footprints are used in this analysis, the proportion of overlap percentages reported here can be interpreted as the proportion of time across the study period that the island is present in those locations. For example, the central (deep purple) sections of Bushy and Masthead show the cay footprint in those locations 90–100 % of the time (Fig. 8d, f), while at Taylor Cay the cay footprints mostly overlap 20–50 % of the time (Fig. 8b). Ecosystem services such as high-value vegetation (e.g., *Pisonia*), require continuous occupation of a considerable proportion of the historical cay positional envelope to maintain these services. Therefore, the results of the RIGAA inform the temporal dynamics and indicate that there is sufficient stable area at both Bushy Islet and Masthead Island to continue to support such high value vegetation communities.

At Masthead Island the maximum historical overlap was 78.1 % indicating that 78.1 % of the historical cay positional envelope is overlapping for the entire observation period (i.e., every cay footprint) between August 2015 and February 2023 (Fig. 8f). At Bushy Islet the maximum historical overlap is 56.9 % (Fig. 8d). The area where all cay footprints overlap is indicative of stable areas of the historical cay positional envelope with Masthead Island being the most stable cay of those studied. Conversely, the sections where the overlap measured <30 % through the observational period relate to the distal spits at the ends of these cays, indicating areas which are both mobile and diverse in their morphological development. The sensitivity of such spits to small changes in the strength and direction of waves and currents is well established (Flood, 1986; Gourlay, 1990; Hopley, 1981). The maximum historical overlap is an important metric to determine a cay's capacity to support permanent ecosystem and cultural services (Albert et al., 2016), while also informing sustainable management of cays by identifying highly dynamic sections of the shoreline. An example of the application of such an investigation is given in Smithers and Dawson (2023) where beach reprofiling at Raine Island was targeted at areas considered stable in the longer-term and corresponded to ecological benefit (in this case facilitating successful turtle nesting). The results for Bushy Islet and Masthead Island indicate that there are large proportions (>50 %) of the historical cay positional envelope which are able to provide ongoing support for ecosystem services.

These findings at Bushy Islet and Masthead Island reflect the behaviour of larger and vegetated cays on the GBR which are less spatially and temporally dynamic when compared to smaller and unvegetated cays (Hamylton and Puotinen, 2015). Fluctuations in the shoreline position around the western distal end of Masthead Island are visible in both the DSAS and RIGAA outputs (Fig. 8e, f) and have previously been observed, suggesting that it is a section most vulnerable to geomorphic change (Edgell, 1928). Considerable spit dynamics have also been observed at the southern end of Bushy Islet which appear to be related to variable wind-wave conditions (Hopley, 1981). Therefore, it is important to note that while there are greater stable proportions of overlap at larger, vegetated cays, they are not exempt from geomorphic change.

At Taylor Cay, there are no areas where 100 % of the cay footprints overlap for the observational period (Fig. 8b, Table 2). The largest proportion of overlap (62.65 %, or 52 of the 83 monthly footprints) represents 3.2 % of the historical cay positional envelope (maximum historical overlap). This indicates a highly dynamic cay in terms of both area and position on the reef platform. Conversely, the SCE result, an average of 63.5 m, for Taylor Cay is misleading suggesting that a proportion of the historical cay positional envelope is in a consistent position for the duration of the analysis period (Fig. 8a). This misleading DSAS result is likely due to the use of a baseline shoreline from which to measure change which is not suitable for dynamic cays. Despite the low proportion overlap and maximum historic overlap metrics showing it is

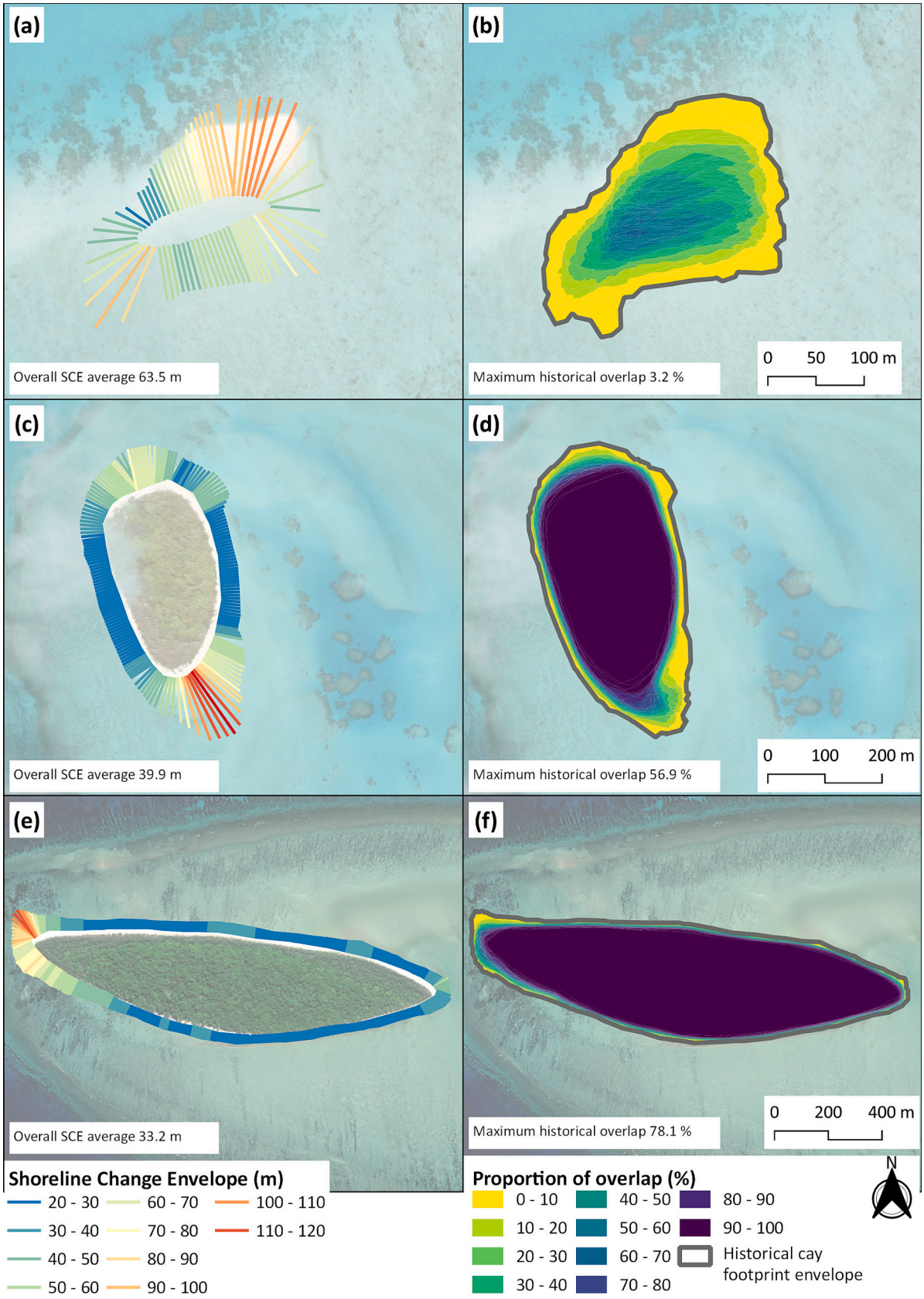

Fig. 8. Comparing DSAS and RIGAA results, respectively, to measure the historical cay footprint intersection for (a, b) Taylor Cay, (c, d) Bushy Islet, and (e, f) Masthead Island. Note: the proportion of overlap is indicated by the graduated colours in (b), (d) and (f), while the maximum historical overlap is indicated intext.

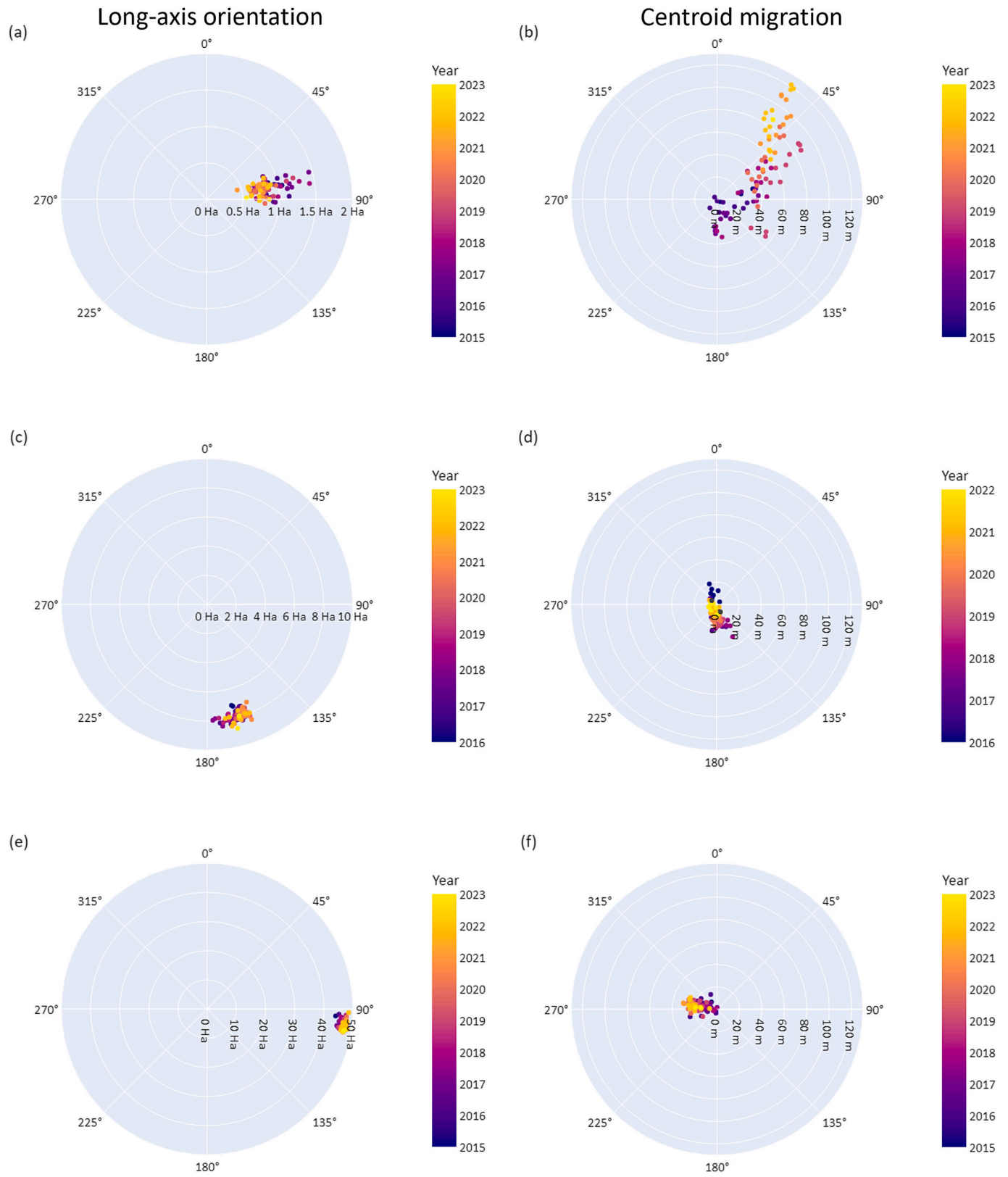

Fig. 9. The monthly long-axis bearing orientation (direction east-west from north) and cay footprint area (Ha) compared with the distance and direction of cay centroid migration for Taylor Cay (a, b), Bushy Islet (c, d) and Masthead Island (e, f). Note: the cay footprint area bands are not uniform in (a), (c) and (e), and the starting year for Bushy Islet is later.

Table 3
Summary comparing the advantages (highlighted green) and disadvantages (highlighted red) of the Reef Island Geomorphic Activity Assessment and the Digital Shoreline Analysis System approaches to assess and measure cay geomorphic change.

Reef Island Geomorphic Activity Assessment	Digital Shoreline Analysis System
Accessible and interpretable to a range of users using open-access software	Requires paid, specialist software
Inherently captures the dynamic nature of the cay shoreline position to calculate metrics	Uses a reference shoreline position which can misrepresent overall cay change
Calculates the spatiotemporal activity of a cay with reference to the historical cay positional envelope which is the total area occupied by the cay over the analysis period.	The use of a reference shoreline can result in misrepresentation of the shoreline change envelope and does not capture the dynamic movement of some cays
Metrics can be meaningfully compared between cays to assist in prioritising monitoring or management works	Metrics are difficult to compare between cays
Metrics inform multiple aspects of cay geomorphic change in a way that is relevant to management interpretation and application	Results are calculated in distances (m) or rates (m/yr) of shoreline change rather than area which may not be meaningful to suitably inform the management of cays and the services they support
Can only be applied to the entire cay shoreline	Can be used to measure change at discrete sections of a cay shoreline

highly dynamic, this does not necessarily mean that ecosystem services like sea bird or turtle nesting cannot be supported by Taylor Cay. Further analysis undertaken around key timeframes (e.g., bird nesting months) would be required to assess the capacity to support ecosystem services at key time periods. The RIGAA metrics reflect the dynamic nature of Taylor Cay, much of which regularly migrates rapidly over the reef flat as wind and wave conditions fluctuate. This behaviour is typical of many unvegetated cays on the GBR (Gourlay, 1983; Hopley, 1978; Taylor, 1924), where the RIGAA methodology could be usefully applied to systematically quantify and compare morphodynamic behaviour and trends.

3.3. Cay orientation and migration

The orientation of a cay's long-axis can rotate in response to external forcings (Cuttler et al., 2020; Flood and Heatwole, 1986). The RIGAA method tracks the oscillations of the cay long-axis orientation. The long-axis orientation of Taylor Cay is easterly oscillating between 68 and 94° (Fig. 9a, Table 2). While there is a marked reduction in cay area over the observation period from 0.8 to 0.55 ha which corresponds with the net contraction findings of the net cay change metric (Fig. 7b) there is no associated change in orientation. These findings suggest that Taylor Cay is undergoing net contraction, rather than fluctuating around an equilibrium morphology, which could indicate a permanent shift in the overall geomorphic change trajectory.

Bushy Islet is orientated north-south between 158 and 177° (Fig. 9c, Table 2). This small range of long-axis orientation may be influenced by the presence of the southern spit which is present <30 % of the time (Fig. 8d). Masthead Island demonstrates an even smaller range of easterly long-axis oscillations between 91 and 100° (Fig. 9e, Table 2). This slight long-axis rotation of Masthead Island may be influenced by the western spit which is spatiotemporally variable (Fig. 8f). Overall, by tracking the angles of long-axis orientation the RIGAA provides an additional indication of the cay dynamics and the response of these cays to external driving forces, such as hydrodynamic conditions (Bonesso et al., 2020).

Cay migration and potential sediment loss across or over the edge of the reef platform has been linked to modified hydrodynamic and sediment transport processes associated with sea-level rise in several studies (Bramante et al., 2020; Shope et al., 2017), where the location of sediment accumulation and cay position changes as wave refraction and energy vary (Webb and Kench, 2010). The RIGAA method can track and clearly depict cay migrations across a reef platform whereas the DSAS lacks a comparable analysis. Taylor Cay demonstrated the greatest range of migration, the centroid moving 120 m towards the northeast of the reef platform (Fig. 9b, Table 2). Considering this pattern of migration in conjunction with net cay contraction, the behaviour of Taylor Cay suggests a gradual redistribution of material over the reef platform and relocation of the cay over time. Additionally, changing hydrodynamic conditions may result in contraction (as seen in Fig. 7b) where there is insufficient energy to transport all the redistributed material up on to the cay or material is permanently lost off the edge of the reef platform. However, as the RIGAA and DSAS only account for cay planimetric change, further volumetric analysis would be required to measure if the total amount of sediment composing the cay has decreased. Bushy Islet and Masthead Island exhibit smaller migration ranges of up to 32 m towards the south and 30 m towards the west, respectively (Fig. 9d, f, Table 2). These findings are more likely to be influenced by the spatiotemporally variable spits at these cays causing a fluctuation in centroid position corresponding to the presence/absence of these spits. A more detailed understanding of the geomorphic controls across a spectrum of environmental and hydrodynamic settings is necessary to infer local and regional influences of cay migration and orientation, and the RIGAA method will provide a standardised approach to accurately quantify cay movements and further develop this understanding, the merits of which are quantitatively summarised in Table 2. Measuring cay orientation and migration is useful to understand the direction and magnitude of processes that drive geomorphic change.

Our new RIGAA approach offers a flexible, comprehensive and multifaceted quantification of cay geomorphic change which is applicable to both relatively stable and dynamic cays. However, the merit of DSAS should not be discounted; it remains useful where the aim is to

measure the distance of shoreline retreat or accretion, or the geomorphic change along a particular section of shoreline is of interest. A qualitative comparison of the RIGAA and DSAS metrics is provided in Table 3. The heterogeneity of our results characterising monthly cay geomorphic activity at three cays shows they can have highly dynamic footprints which are important for users to meaningfully measure to resolve whether perturbations are of a greater magnitude than usual or if they represent longer-term trends. Further investigation into the geomorphic settings which lead to varied cay behaviour is required to classify cays more broadly and systematically within the GBR. The findings from this study show how RIGAA provides meaningful and quantitative outputs which enable users to understand cay geomorphic change over episodic, seasonal and interannual timescales (i.e., the user's timeframe of interest). The outputs can be used to inform the appropriate and sustainable management of the valuable ecosystem and cultural services that cays support. Finally, the RIGAA method can be tailored by the user to the timeframe of interest and be applied to the most suitable shoreline proxy based on the study setting (e.g., TOB, vegetation line or mean sea level).

4. Conclusion

The Reef Island Geomorphic Activity Assessment (RIGAA) approach offers a high spatiotemporal resolution method to quantify and compare cay geomorphic behaviour applicable to global reef island settings. The RIGAA metrics provide a more quantitative and thorough understanding of cay shoreline and positional change. These metrics are more relevant to managers than existing approaches, such as DSAS. The improved metrics offered by RIGAA can be used to identify cays where net cay change (e.g., net contraction), indicates that management intervention may be required then quantify the spatiotemporal scale of cay morphodynamics (using the historical cay footprint intersection metrics) to inform appropriate and sustainable cay management to preserve ecosystem and cultural services supported by cays. Finally, the cay orientation and migration metrics can inform the short- to long-term response of the cay to external conditions, such as variable hydrodynamic conditions. The RIGAA is an easily adaptable approach with outputs that are accessible to a range of users.

Supplementary data to this article can be found online at https://doi.org/10.1016/j.gloplacha.2025.104743.

CRediT authorship contribution statement

Emily Lazarus: Writing – original draft, Visualization, Validation, Methodology, Investigation, Data curation, Conceptualization. **Stephanie Duce:** Writing – original draft, Visualization, Supervision, Methodology, Conceptualization. **Stephen Lewis:** Writing – original draft, Supervision, Conceptualization. **Scott Smithers:** Writing – original draft, Visualization, Supervision, Methodology, Conceptualization.

Declaration of competing interest

The authors declare the following financial interests/personal relationships which may be considered as potential competing interests:

Emily Lazarus reports financial support was provided by Commonwealth of Australia. If there are other authors, they declare that they have no known competing financial interests or personal relationships that could have appeared to influence the work reported in this paper.

Acknowledgements

This study was supported by an Australian Government Research Training Program Scholarship. The funding source had no involvement in the study.

Data availability

Data will be made available on request.

References

Adnan, F.A.F., Hamylton, S.M., Woodroffe, C.D., 2016. A Comparison of shoreline changes estimated using the Base of Beach and Edge of Vegetation Line at North Keeling Island. J. Coast. Res. 75 (sp1), 967–971. https://doi.org/10.2112/SI75-194.1.

Albert, S., Leon, J.X., Grinham, A.R., Church, J.A., Gibbes, B.R., Woodroffe, C.D., 2016. Interactions between sea-level rise and wave exposure on reef island dynamics in the Solomon Islands. Environ. Res. Lett. 11 (5), 54011. https://doi.org/10.1088/1748-9326/11/5/054011.

Bishop-Taylor, R., Nanson, R., Sagar, S., Lymburner, L., 2021. Mapping Australia's dynamic coastline at mean sea level using three decades of Landsat imagery. Remote Sens. Environ. 267, 112734. https://doi.org/10.1016/j.rse.2021.112734.

BOM, 2023. ENSO Outlook: An alert system for the El Niño-Southern Oscillation. Retrieved 06/12/2023 from. http://www.bom.gov.au/climate/enso/outlook/.

Bonesso, J.L., Cuttler, M.V.W., Browne, N., Hacker, J., O'Leary, M., 2020. Assessing Reef Island Sensitivity based on LiDAR-Derived Morphometric Indicators. Remote Sens. (Basel, Switzerland) 12 (18), 3033. https://doi.org/10.3390/rs12183033.

Bramante, J.F., Ashton, A.D., Storlazzi, C.D., Cheriton, O.M., Donnelly, J.P., 2020. Sea level rise will drive divergent sediment transport patterns on fore reefs and reef flats, potentially causing erosion on atoll islands. J. Geophys. Res. Earth 125 (10), n/a. https://doi.org/10.1029/2019JF005446.

Costa, M.B., Macedo, E.C., Siegle, E., 2017. Planimetric and volumetric changes of reef islands in response to wave conditions: Planimetric and volumetric changes of reef islands. Earth Surf. Process. Landf. 42 (15), 2663–2678. https://doi.org/10.1002/esp.4215.

Cuttler, M.V.W., Vos, K., Branson, P., Hansen, J.E., O'Leary, M., Browne, N., Lowe, R., 2020. Interannual response of reef islands to climate-driven variations in water level and wave climate. Remote Sens. (Basel, Switzerland) 12 (24), 4089. https://doi.org/10.3390/rs12244089.

Dawson, J.L., 2021. Multi-decadal shoreline morphodynamics of a shelf-edge reef island, Great Barrier Reef; implications for future island persistence. Geomorphology (Amsterdam, Netherlands) 392, 107920. https://doi.org/10.1016/j.geomorph.2021.107920.

Duvat, V.K.E., 2019. A global assessment of atoll island planform changes over the past decades. Wiley interdisciplinary reviews. Climate Change 10 (1). https://doi.org/10.1002/wcc.557 e557-n/a.

Duvat, V.K.E., Pillet, V., 2017. Shoreline changes in reef islands of the Central Pacific; Takapoto Atoll, northern Tuamotu, French Polynesia. Geomorphology (Amsterdam, Netherlands) 282, 96–118. https://doi.org/10.1016/j.geomorph.2017.01.002.

Edgell, J., 1928. Changes at Masthead Island. Reports Great Barrier Reef Commit. 2, 57.

ESA, 2012. Sentinel-2: ESA's Optical High-Resolution Mission for GMES Operational Services (ESA SP-1322/2 March 2012). https://sentinel.esa.int/documents/247904/349490/s2_sp-1322_2.pdf.

Flood, P., 1974. Sand movements on Heron Island- a vegetated sand cay Great Barrier Reef Province, Australia. In: Proceedings of the Second International Symposium on Coral Reefs.

Flood, P., 1986. Sensitivity of coral cays to climatic variations, southern Great Barrier Reef, Australia. Coral Reefs: J. Intern. Soc. Reef Stud. 5 (1), 13–18. https://doi.org/10.1007/BF00302166.

Flood, P.G., Heatwole, H., 1986. Coral Cay Instability and Species-turnover of Plants at Swain Reefs, Southern Great Barrier Reef, Australia. J. Coast. Res. 2 (4), 479–496.

Ford, M., 2012. Shoreline changes on an Urban Atoll in the Central Pacific Ocean: Majuro Atoll, Marshall Islands. J. Coast. Res. 28 (1), 11–22. https://doi.org/10.2112/JCOASTRES-D-11-00008.1.

Ford, M., 2013. Shoreline changes interpreted from multi-temporal aerial photographs and high resolution satellite images: Wotje Atoll, Marshall Islands. Remote Sens. Environ. 135, 130–140. https://doi.org/10.1016/j.rse.2013.03.027.

Gourlay, M., Baker, J.T., Carter, R.M., Sammarco, P.W., Stark, K.P., 1983. Accretion and erosion of coral cays and some consequent implications for the management of Marine Parks. In: Proceedings of the Great Barrier Reef Conference', Townsville.

Gourlay, M., 1990. Waves, Set-up and Currents on Reefs: Cay Formation and Stability. Proceedings of the Conference on Engineering in Coral Reef Regions, Townsville.

Gourlay, M.R., 1988. Coral cays: Products of wave action and geological processes in a biogenic environment. In: Proceedings of the 6th International Coral Reef Symposium, Australia, vol. 2, pp. 491–496.

Hamylton, S., Puotinen, M., 2015. A meta-analysis of reef island response to environmental change on the Great Barrier Reef. Earth Surf. Process. Landf. 40 (8), 1006–1016. https://doi.org/10.1002/esp.3694.

Hamylton, S.M., 2017. Mapping coral reef environments: a review of historical methods, recent advances and future opportunities. Prog. Phys. Geogr. 41 (6), 803–833. https://doi.org/10.1177/0309133317744998.

Himmelstoss, E.A., Henderson, R.E., Kratzmann, M.G., Farris, A.S., 2018. Digital Shoreline Analysis System (DSAS) Version 5.0 user Guide (2331-1258).

Holdaway, A., Ford, M., 2019. Resolution and scale controls on the accuracy of atoll island shorelines interpreted from satellite imagery. Appl. Geomat. 11 (4), 339–352. https://doi.org/10.1007/s12518-019-00266-7.

Hopley, D., 1978. Geographical Studies of the Townsville Area. Dept. of Geography, James Cook Univ.

Hopley, D., 1981. Sediment Movement around a Coral Cay. Great Barrier Reef, Australia.

Husband, E., East, H.K., Hocking, E.P., Guest, J., 2023. Honduran Reef Island shoreline change and planform evolution over the last 15 years: implications for Reef Island monitoring and futures. Remote Sens. (Basel, Switzerland) 15 (19), 4787. https://doi.org/10.3390/rs15194787.

Jenkins, K., 2020. In: Jenkins, K. (Ed.), QGIS Count Polygon Overlap Model. https://github.com/kgjenkins/qgis-count-polygon-overlap/tree/main.

Kench, P., Brander, R., 2006. Response of reef island shorelines to seasonal climate oscillations; South Maalhosmadulu Atoll, Maldives. J. Geophys. Res. 111 (F1). https://doi.org/10.1029/2005JF000323. F01001-n/a.

Kench, P., Liang, C., Ford, M., Owen, S., Aslam, M., Ryan, E., Turner, T., Beetham, E., Dickson, M., Stephenson, W., 2023. Reef islands have continually adjusted to environmental change over the past two millennia. Nat. Commun. 14 (1), 508.

Kennedy, D.M., 2024. A review of the vulnerability of low-lying reef island landscapes to climate change and ways forward for sustainable management. Ocean Coast. Manag. 249, 106984. https://doi.org/10.1016/j.ocecoaman.2023.106984.

Lowe, M.K., Adnan, F.A.F., Hamylton, S.M., Carvalho, R.C., Woodroffe, C.D., 2019. Assessing Reef-Island shoreline Change using UAV-Derived orthomosaics and digital surface models. Drones 3 (2), 44. https://www.mdpi.com/2504-446X/3/2/44.

Mann, T., Westphal, H., 2016. Multi-decadal shoreline changes on Taku Atoll, Papua New Guinea; observational evidence of early reef island recovery after the impact of storm waves. Geomorphology (Amsterdam, Netherlands) 257, 75–84. https://doi.org/10.1016/j.geomorph.2015.12.028.

Mann, T., Bayliss-Smith, T., Westphal, H., 2016. A geomorphic interpretation of shoreline change rates on Reef Islands. J. Coast. Res. 32 (3), 500–507. https://doi.org/10.2112/JCOASTRES-D-15-00093.1.

Paris, P., Mitasova, H., 2014. Barrier Island dynamics using mass center analysis: a new way to detect and track large-scale change. ISPRS Int. J. Geo Inf. 3 (1), 49–65. https://doi.org/10.3390/ijgi3010049.

Purkis, S.J., Gardiner, R., Johnston, M.W., Sheppard, C.R.C., 2016. A half century of coastline change in Diego Garcia; the largest atoll island in the Chagos. Geomorphology (Amsterdam, Netherlands) 261, 282–298. https://doi.org/10.1016/j.geomorph.2016.03.010.

Sengupta, M., Ford, M.R., Kench, P.S., 2021. Multi-decadal planform changes on coral reef islands from atolls and mid-ocean reef platforms of the Equatorial Pacific Ocean; Gilbert Islands, Republic of Kiribati. Geomorphology (Amsterdam, Netherlands) 389, 107831. https://doi.org/10.1016/j.geomorph.2021.107831.

Shope, J.B., Storlazzi, C.D., 2019. Assessing morphologic controls on atoll island alongshore sediment transport gradients due to future sea-level rise. Front. Mar. Sci. 6. https://doi.org/10.3389/fmars.2019.00245.

Shope, J.B., Storlazzi, C.D., Hoeke, R.K., 2017. Projected atoll shoreline and run-up changes in response to sea-level rise and varying large wave conditions at Wake and Midway Atolls, northwestern Hawaiian Islands. Geomorphology (Amsterdam, Netherlands) 295, 537–550. https://doi.org/10.1016/j.geomorph.2017.08.002.

Smithers, S.G., Dawson, J.L., 2023. Beach reprofiling to improve reproductive output at the world's largest remaining green turtle rookery: Raine Island, northern Great Barrier Reef. Ocean Coast. Manag. 231, 106385. https://doi.org/10.1016/j.ocecoaman.2022.106385.

Steers, J., 1929. The Queensland Coast and the Great Barrier Reefs. Geogr. J. 74 (3), 232–257. https://doi.org/10.2307/1784362.

Stoddart, D., McLean, R., Hopley, D., 1978. Geomorphology of reef islands, northern Great Barrier Reef. Philos. Trans. R. Soc. Lond. Ser. B Biol. Sci. 284 (999), 39–61. https://doi.org/10.1098/rstb.1978.0052.

Stoddart, D.R., 1962. Three Caribbean Atolls: Turneffe Islands, Lighthouse Reef, and Glover's Reef. British Honduras. Atoll Research Bulletin.

Taylor, T., 1924. Movement of sand cays. Queensl. Geograph. J. 39, 38–39.

Terres de Lima, L., Fernández-Fernández, S., de Almeida, Marcel, Espinoza, J., da Guia Albuquerque, M., Bernardes, C., 2021. End Point Rate Tool for QGIS (EPR4Q): Validation using DSAS and AMBUR. ISPRS Int. J. Geo Inf. 10 (3), 162. https://doi.org/10.3390/ijgi10030162.

Umbgrove, J.H.F., 1928. De koraalriffen van den Spermonde- Archipel (Zuid-Celebes). Leidse. Geol. Meded. 3 (1), 228–247.

Webb, A.P., Kench, P.S., 2010. The dynamic response of reef islands to sea-level rise; evidence from multi-decadal analysis of island change in the Central Pacific. Glob. Planet. Chang. 72 (3), 234–246. https://doi.org/10.1016/j.gloplacha.2010.05.003.